

One-way invisible cloak using parity-time symmetric transformation optics

Xuefeng Zhu,^{1,2} Liang Feng,¹ Peng Zhang,¹ Xiaobo Yin,^{1,3} and Xiang Zhang^{1,3,*}

¹NSF Nanoscale Science and Engineering Center, 3112 Etcheverry Hall, University of California, Berkeley, California 94720, USA

²Huazhong University of Science and Technology, Wuhan, Hubei 430074, China

³Materials Science Division, Lawrence Berkeley National Laboratory, 1 Cyclotron Road, Berkeley, California 94720, USA

*Corresponding author: xiang@berkeley.edu

Received May 22, 2013; revised July 2, 2013; accepted July 4, 2013;
posted July 8, 2013 (Doc. ID 191018); published July 29, 2013

We propose a one-way invisible cloak using transformation optics of parity-time (*PT*) symmetric optical materials. At the spontaneous *PT*-symmetry breaking point, light is scattered only for incidence along one direction since the phase-matching condition is unidirectionally satisfied, making the cloak one-way invisible. Moreover, optical scattering from the one-way cloak can be further engineered to realize more interesting effects, for example, creating a unidirectional optical illusion of the concealed object. © 2013 Optical Society of America

OCIS codes: (160.3918) Metamaterials; (230.3205) Invisibility cloaks; (290.5839) Scattering, invisibility.
<http://dx.doi.org/10.1364/OL.38.002821>

In the past few years, considerable research efforts have been investigated in transformation optics to develop a variety of devices with unprecedented performances [1–11]. Using the coordinate transformation to map the distributions of permittivity and permeability from a virtual space to a physical space, myriad exotic effects such as invisibility cloaking become possible [3,8,11]. The previous studies were mainly focused on the perfect cloaks to make the concealed object omnidirectionally invisible to the outside observers [1,9]. In many cases, however, it might be important to have the cloak selectively visible for only one direction, i.e., a one-way cloak. It has been proposed using a coordinate-transformed nonreciprocal photonic crystal in which reciprocity of light is broken by creating an asymmetric permeability tensor with an external magnetic field [12]. Nevertheless, a one-way cloak without applying a static magnetic field is more desirable for optical devices and applications. Recently, by engineering the complex dielectric permittivity plane in its entirety, parity-time (*PT*) symmetric potentials have been constructed to achieve unidirectional light transport: for example, one-way invisibility has been demonstrated at the spontaneous *PT* symmetry breaking point (also called the exceptional point) [13–20]. The observed unidirectional invisibility from the *PT* symmetric potentials provides an efficient approach to achieving one-way invisible cloaks, complementing so far explored omnidirectional cloaks.

In this Letter, by introducing the *PT* symmetric optical potentials into transformation optics, we propose a new scheme to realize the one-way invisible cloak. Since the transformed *PT* symmetric potentials provide a specific unidirectional wave vector, unidirectional light reflection and scattering are expected to occur when the phase-matching condition is satisfied, while light incident from the other direction propagates through the potentials without any perturbation. Therefore, the concealed object is cloaked depending on incident directions of light. Moreover, we show that the enhanced backward scattering from the transformed *PT* symmetric potentials can be engineered to demonstrate a one-way optical illusion of the concealed object.

The corresponding coordinate transformation between physical and virtual spaces is given by $\epsilon' = A\epsilon A^T / \det A$ and $\mu' = A\mu A^T / \det A$ [1], where ϵ (or μ) and ϵ' (or μ') denote the permittivity (or permeability) in the virtual space x and the physical space x' , respectively, and A is the Jacobian matrix with components of $A_{ij} = h'_i \partial x'_i / h_i \partial x_i$.

Here, a pushing-forward coordinate mapping is applied to expand a point to a circular hole with $r = f(r') = b(r' - a)/(b - a)$ and $\theta = \theta'$ in polar coordinates [1], as shown in Fig. 1(a), where the singularity at the boundary of the circular hole limits the operating bandwidth of the transformed *PT* cloak [1,2], even though *PT* symmetric potentials have a broadband unidirectional response. In the virtual space ($r \leq b$), a *PT* symmetric potential is constructed with a periodic complex modulation in its permittivity: $\epsilon = 1 + \zeta \exp(i\beta r \cos \theta)$, where ζ is the modulation amplitude and β is the modulation vector, respectively, as shown in Fig. 1(b). For transverse electric (TE)-polarized light, ϵ' and μ' in the physical space ($a \leq r' \leq b$) after transformation is written as

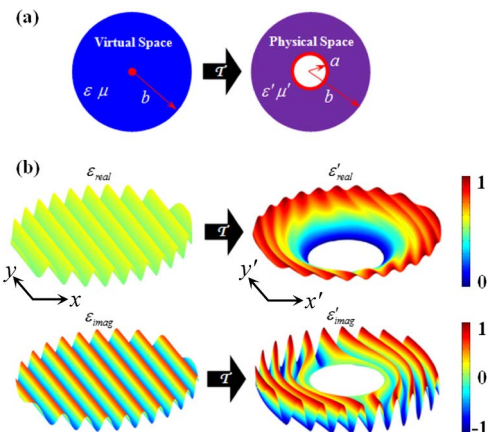


Fig. 1. (a) Coordinate transformation to expand the red point ($r = 0$) in the virtual space ($r \leq b$) to a hollow hole ($r' \leq a$) in the physical space ($a \leq r' \leq b$). (b) Corresponding complex permittivities of the *PT* symmetric potential in virtual and physical spaces, respectively.

$\varepsilon'_z = f(r')f'(r')\varepsilon_{f(r'),\theta}/r'$, $\mu'_{r'} = f(r')\mu/[r'f'(r')]$, and $\mu'_{\theta'} = f^2(r')r'\mu/f(r')$, in which the corresponding permeability tensor is anisotropic and inhomogeneous. Metamaterial design might be required to realize such magnetic responses at optical frequencies [21,22]. Moreover, the associated material anisotropy and inhomogeneity can be achieved through the hyperbolic metamaterials [23]. It is worth noting that different from the one-way cloak in [12], the resulting permeability tensor in our cloak is still symmetric such that no external magnetic field is required to achieve the one-way effect.

The total electric field including both incident and scattered fields (E_{in} and E_{sc}) is expressed as

$$E_z = E_{\text{in}}(x) \exp(ik_1x) + E_{\text{sc}}(x) \exp(ik_2x). \quad (1)$$

By substituting Eq. (1) into the Helmholtz equation, a coupled-mode equation can be obtained. For convenience, a phase-matching factor is defined as $\delta = \beta + k_1 - k_2$, where k_1 and k_2 represent the wave vectors of the incident and scattered light, respectively. If $\delta = 0$ where the phase-matching condition is perfectly satisfied, the coupled-mode equation is reduced to [16]

$$\begin{bmatrix} \frac{dE_{\text{in}}}{dx} \\ \frac{dE_{\text{sc}}}{dx} \end{bmatrix} = \begin{bmatrix} i\frac{\omega^2\zeta}{2k_1c^2} \exp(i\beta x) & i\frac{\omega^2\zeta}{2k_1c^2} \exp[i2\beta x] \\ i\frac{\omega^2\zeta}{2k_2c^2} & i\frac{\omega^2\zeta}{2k_2c^2} \exp(i\beta x) \end{bmatrix} \begin{bmatrix} E_{\text{in}} \\ E_{\text{sc}} \end{bmatrix}, \quad (2)$$

where the fast oscillating terms $\exp(i\beta x)$ and $\exp(i2\beta x)$ have no contributions since their averages over a modulation period are zero, thus leading to a simplified form

$$\frac{dE_{\text{in}}}{dx} = 0, \quad \frac{dE_{\text{sc}}}{dx} = i\frac{\omega^2\zeta}{2k_2c^2} E_{\text{in}}. \quad (3)$$

In our study, the initial conditions for incident and scattered fields are $E_{\text{in}} \neq 0$ and $E_{\text{sc}} = 0$, respectively. For a specific incident light with a wave vector of k_1 , if the phase-matching condition is satisfied, i.e., $\delta \approx 0$, the wave vector of the scattered light is thus $k_2 \approx \beta + k_1$. From Eq. (3), it is evident that E_{sc} increases linearly as propagating inside the PT symmetric potential while E_{in} remains unchanged. On the other hand, if $\delta \neq 0$, the overall energy transfer to the scattered components is negligible due to the phase mismatch, and E_{sc} thus remains almost 0.

Finite element method simulations were then implemented to validate the proposed one-way invisibility of transformed PT symmetric potentials. In simulations, as shown in Fig. 2, the TE-polarized plane wave is incident from both left [Figs. 2(a) and 2(c)] and right [Figs. 2(b) and 2(d)] directions. The operating wavelength is set $\lambda = 0.1$ unit. Therefore, to form the strong Bragg reflection, the modulation vector of the PT potential in the virtual space is $\beta = 4\pi/\lambda$. The corresponding parameters in the circular region ($|x| \leq 2.5\lambda$) [see Figs. 2(a) and 2(b)] are then $\varepsilon = 1 + 0.1 \exp(i125.66x)$ and $\mu = 1$. In Fig. 2(a), for left incidence, strong Bragg reflection is visualized due to the satisfied phase-matching condition $k_2 \approx \beta + k_1$ [see the inset vector diagram of Fig. 1(a)]; whereas for right incidence in Fig. 2(b), scattered light

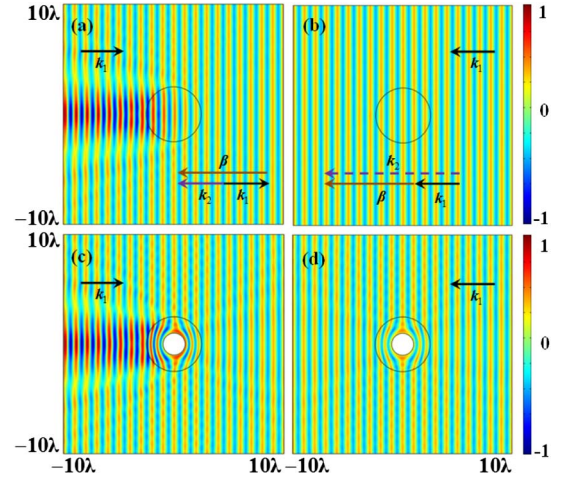


Fig. 2. Numerical mappings of the total electric field in (a), (b) the virtual space and (c), (d) the physical space. In (a) and (c) where light is incident from left, strong backscattered reflection can be clearly observed because of the satisfied phase matching. However, in (b) and (d) where light is incident from right, phase is mismatched and thus light propagates without exciting any scattered light.

is barely observed since the corresponding vector diagram shows that k_2 will be larger than k_1 and thus fall into the evanescent regime. The results in our simulations are consistent with the reported unidirectional invisibility [17–20].

Figures 2(c) and 2(d) are the corresponding simulations of the PT cloak in the physical space after coordinate transformation, where a perfect electric conductor (PEC) cylinder with a radius of λ is concealed and one-way cloaked. Overall, the field distributions in both directions agree well with the results in the virtual space [Figs. 2(a) and 2(b)] despite a small amount of scattering caused by the singularity at the boundary of the PEC cylinder $|x'| = \lambda$. Additionally, the total power in the whole simulation domain grows as wave propagates though the PT potential, which, however, does not violate the energy conservation law since optical gain in the PT potential provides additional power.

In Figs. 3(a) and 3(b), the scattering pattern of a PEC cylinder is numerically mapped for a point source located at $(-5\lambda, 0)$ and $(5\lambda, 0)$, respectively. When the PEC cylinder is shielded by the PT cloak, the one-way invisibility effect can also be clearly observed, as shown in Figs. 3(c) and 3(d). In Fig. 3(d), an undisturbed cylindrical wave pattern is presented in the far field on both sides of the cloak, indicating excellent cloaking effect as the expected phase mismatch indeed forbids the energy transfer to the scattered components. It is worth noting that even if the point source is located left to the cloak as shown in Fig. 3(c) in which reflection is induced, the concealed PEC cylinder also remains invisible to the observer standing right to the PT cloak. This is due to the fact that the designed phase matching is only valid for reflection. Therefore, with no contribution from scattering in light transmission as expected from Eq. (3), field distribution after the PT cloak remains the same as that from the point source. However, while the observer behind the PT cloak sees unperturbed light propagation,

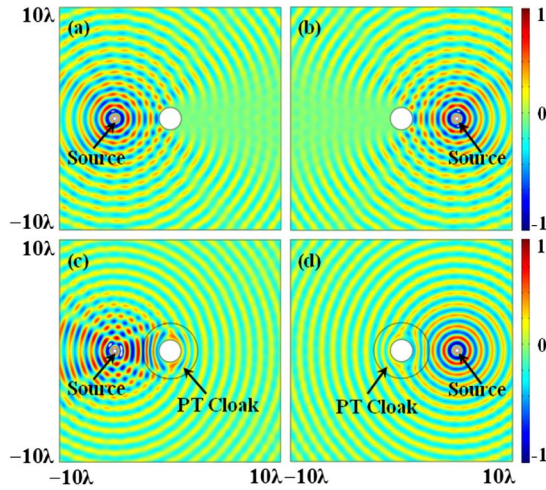


Fig. 3. Numerical mappings of the total electric field with a TE-polarized point source impinging on a PEC cylinder ($r' \leq \lambda$) (a), (b) without and (c), (d) with the PT cloak ($\lambda \leq r' \leq 2.5\lambda$). The point source is located at (a), (c) $(-5\lambda, 0)$ and (b), (d) $(5\lambda, 0)$, respectively. The radius of the source is 0.2λ .

the one in front may have an illusion that light is reflected back from a concave mirror.

We further compared the scattering patterns from the cloaked PEC cylinder and a PEC concave mirror, as shown in Fig. 4. In Fig. 4(a), the normalized scattering fields of the cloaked PEC cylinder are plotted with different illumination conditions of TE-polarized cylindrical light, where the point source is located at $(-3\lambda, 0)$, $(-5\lambda, 0)$, and $(-7\lambda, 0)$, respectively. The results clearly indicate that the backward scattering angle becomes narrower as the source is moved away from the concealed object. These backscattering patterns from the PT cloak are almost equivalent to those from a PEC concave mirror, creating an illusion in reflection as if there existed a PEC concave mirror instead of the concealed PEC cylinder, as shown in Fig. 4(b). Moreover, simulated field distributions, shown in Figs. 4(c) and 4(d), further confirm the resemblance of scattered fields between two cases. It is evident that great consistency in both amplitude and phase of backscattering has been achieved nearby the point source. Similar to the demonstrated one-way cloak in Figs. 2 and 3, such an optical illusion is also unidirectional for the point source located left to the PT cloak.

In summary, we have demonstrated a new type of one-way invisible cloak using a transformed PT symmetric optical potential at the spontaneous PT symmetry breaking point. For one direction that satisfies the phase-matching condition, light is strongly reflected, while light remains unperturbed if propagating in the other direction. Numerical results have shown that the scattering from the PT cloak can be structured to provide a specific detectable route to the outside world and even give an optical illusion for the concealed object. Moreover, in order to create an arbitrary optical illusion, it will be necessary to engineer the direction, amplitude, and phase of each scattered component, which is possible if a more generalized PT symmetric potential is introduced in the virtual space, i.e., $\Delta\epsilon(x) = \sum_j \zeta_j \exp(i\beta_j \cdot x + i\varphi_j)$. In this case, the amplitude, direction, and phase of the scattered mode (j) can be flexibly tuned with the material

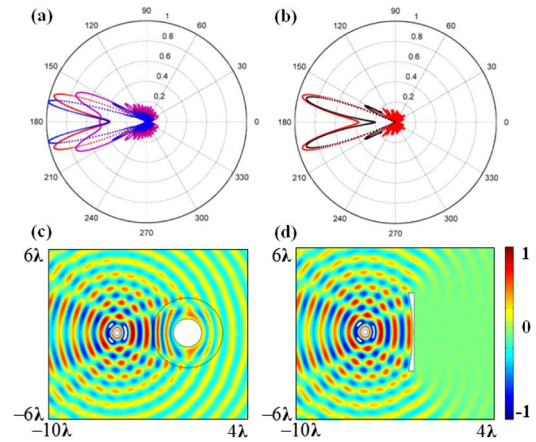


Fig. 4. (a) Purple, red, and blue curves represent the normalized scattering fields of the cloaked PEC cylinder, where the point source is located at $(-3\lambda, 0)$, $(-5\lambda, 0)$, and $(-7\lambda, 0)$, respectively. (b) Comparison of the normalized scattering fields from the cloaked PEC cylinder (red) and a concave PEC mirror (black), where the point source is located at $(-5\lambda, 0)$. (c) and (d) are the corresponding simulated field distributions for the cloaked PEC cylinder and the concave PEC mirror, respectively.

parameters of ζ_j , β_j , and φ_j , respectively, for the given physical size of the illusion device and the wave vector of incident light. By investigating the PT symmetric optical potentials within the context of transformation optics, our scheme offers great material design flexibility and additional freedoms for developing novel photonic devices. In practice, the realization of the proposed one-way invisible cloak might be experimentally realized by transforming the demonstrated unidirectional PT symmetric materials [20]. Compared to the conventional cloaking proposals [1,2], the simultaneous transformations of both real and imaginary parts of the index of refraction in this work may require more sophisticated metamaterial design and engineering [21–23]. Additionally, because of broadband unidirectional performance of PT symmetric materials, one-way hiding of events can be expected if the previously demonstrated space-time cloaking technique is applied [24,25].

This work was supported by the US ARO MURI program (W911NF-09-1-0539). X. F. Zhu acknowledges the financial support from the Bird Nest Plan of HUST.

References

1. J. B. Pendry, D. Schurig, and D. R. Smith, *Science* **312**, 1780 (2006).
2. A. Greenleaf, M. Lassas, and G. Uhlmann, *Phys. Rev. Lett.* **99**, 183901 (2007).
3. W. S. Cai, U. K. Chettiar, A. V. Kildishev, and V. M. Shalaev, *Nat. Photonics* **1**, 224 (2007).
4. A. V. Kildishev and V. M. Shalaev, *Opt. Lett.* **33**, 43 (2008).
5. M. Rahm, D. A. Roberts, J. B. Pendry, and D. R. Smith, *Opt. Express* **16**, 11555 (2008).
6. N. M. Litchinitser, A. I. Maimistov, I. R. Gabitov, R. Z. Sagdeev, and V. M. Shalaev, *Opt. Lett.* **33**, 2350 (2008).
7. J. Li and J. B. Pendry, *Phys. Rev. Lett.* **101**, 203901 (2008).
8. J. Valentine, J. Li, T. Zentgraf, G. Bartal, and X. Zhang, *Nat. Mater.* **8**, 568 (2009).
9. U. Leonhardt and T. Tyc, *Science* **323**, 110 (2009).

10. Y. Lai, J. Ng, H. Y. Chen, D. Z. Han, J. J. Xiao, Z. Q. Zhang, and C. T. Chan, *Phys. Rev. Lett.* **102**, 253902 (2009).
11. M. Gharghi, C. Gladden, T. Zentgraf, Y. M. Liu, X. B. Yin, J. Valentine, and X. Zhang, *Nano Lett.* **11**, 2825 (2011).
12. C. He, X. L. Zhang, L. Feng, M. H. Lu, and Y. F. Chen, *Appl. Phys. Lett.* **99**, 151112 (2011).
13. S. Longhi, *Phys. Rev. Lett.* **103**, 123601 (2009).
14. C. E. Rüter, K. G. Makris, R. El-Ganainy, D. N. Christodoulides, M. Segev, and D. Kip, *Nat. Phys.* **6**, 192 (2010).
15. C. T. West, T. Kottos, and T. Prosen, *Phys. Rev. Lett.* **104**, 054102 (2010).
16. Y. D. Chong, L. Ge, and A. D. Stone, *Phys. Rev. Lett.* **106**, 093902 (2011).
17. L. Feng, M. Ayache, J. Huang, Y. L. Xu, M. H. Lu, Y. F. Chen, Y. Fainman, and A. Scherer, *Science* **333**, 729 (2011).
18. Z. Lin, H. Ramezani, T. Eichelkraut, T. Kottos, H. Cao, and D. N. Christodoulides, *Phys. Rev. Lett.* **106**, 213901 (2011).
19. A. Regensburger, C. Bersch, M. A. Miri, G. Onishchukov, D. N. Christodoulides, and U. Peschel, *Nature* **488**, 167 (2012).
20. L. Feng, Y. L. Xu, W. S. Fegadolli, M. H. Lu, J. B. E. Oliveira, V. Almeida, Y. F. Chen, and A. Scherer, *Nat. Mater.* **12**, 108 (2013).
21. A. N. Grigorenko, A. K. Geim, H. F. Gleeson, Y. Zhang, A. A. Firsov, I. Y. Khrushchev, and J. Petrovic, *Nature* **438**, 335 (2005).
22. V. M. Shalaev, *Nat. Photonics* **1**, 41 (2007).
23. D. R. Smith and D. Schurig, *Phys. Rev. Lett.* **90**, 077405 (2003).
24. M. W. McCall, A. Favaro, P. Kinsler, and A. Boardman, *J. Opt.* **13**, 024003 (2011).
25. M. Fridman, A. Farsi, Y. Okawachi, and A. L. Gaeta, *Nature* **481**, 62 (2012).